Crystal structures of hevamine, a plant defence protein with chitinase and lysozyme activity, and its complex with an inhibitor

Terwisscha van Scheltinga, Anke C.; Kalk, Kor H.; Beintema, Jaap J.; Dijkstra, Bauke W.

Published in:
Structure

DOI:
10.1016/S0969-2126(94)00120-0

Publication date:
1994

Crystal structures of hevamine, a plant defence protein with chitinase and lysozyme activity, and its complex with an inhibitor

Anke C Terwisscha van Scheltinga[1], Kor H Kalk[1], Jaap J Beintema[2] and Bauke W Dijkstra[1]*

[1]BIOSON Research Institute and Laboratory of Biophysical Chemistry, Department of Chemistry, University of Groningen, Nijenborgh 4, 9747 AG Groningen, The Netherlands and [2]Laboratory of Biochemistry, Department of Chemistry, University of Groningen, Nijenborgh 4, 9747 AG Groningen, The Netherlands

Background: Hevamine is a member of one of several families of plant chitinases and lysozymes that are important for plant defence against pathogenic bacteria and fungi. The enzyme can hydrolyze the linear polysaccharide chains of chitin and peptidoglycan. A full understanding of the structure/function relationships of chitinases might facilitate the production of transgenic plants with increased resistance towards a wide range of pathogens.

Results: The crystal structure of hevamine has been determined to a resolution of 2.2 Å, and refined to an R-factor of 0.169. The enzyme possesses a $(\beta\alpha)_8$-barrel fold. An inhibitor binding study shows that the substrate-binding cleft is located at the carboxy-terminal end of the β-barrel, near the conserved Glu127. Glu127 is in a position to act as the catalytic proton donor, but no residue that might stabilize a positively charged oxocarbonium ion intermediate was found. A likely mechanism of substrate hydrolysis is by direct attack of a water molecule on the C1 atom of the scissile bond, resulting in inversion of the configuration at C1.

Conclusions: The structure of hevamine shows a completely new lysozyme/chitinase fold and represents a new class of polysaccharide-hydrolyzing $(\beta\alpha)_8$-barrel enzymes. Because the residues conserved in the family to which hevamine belongs are important for maintaining the structure of the $(\beta\alpha)_8$-barrel, all members of the family, including fungal, bacterial and insect chitinases, are likely to share this architecture. The crystal structure obtained provides a basis for protein engineering studies in this family of chitinases.

Structure 15 December 1994, **2**:1181–1189

Key words: glycosyl hydrolase, pathogenesis-related proteins, TIM barrel, X-ray structure

Introduction

Many plants produce chitinases and other so-called pathogenesis-related proteins to deal with stressful conditions such as wounding and pathogen attack (for reviews, see [1,2]). Chitinases are enzymes that can hydrolyze chitin, a long linear chain of β(1,4)-linked *N*-acetylglucosamine residues. Chitin is a major component of the cell wall of fungi and the exoskeleton of arthropods. It is thought that the chitinases provide the plant with a defence mechanism against fungi and insects. Indeed, it has been shown that chitinases from bean leaves inhibit fungal growth *in vitro* [3]. Moreover, some transgenic plants that over-expressed chitinase showed an increased resistance to several chitinous pathogens. Not all such experiments yielded positive results, however [1], and it has been suggested that significant protection might require the combined high-level expression of both chitinase and glucanase as both have been shown to act synergistically *in vitro* [4].

Plants produce both intracellular and extracellular chitinases that all have a molecular weight of 25–35 kDa [1]. Characterization and sequence determination of these plant chitinases revealed the existence of two major families, which can be subdivided into five classes [5]. According to the classification of glycosyl hydrolases introduced by Henrissat [6,7], chitinase classes I, II and IV belong to family 19, and classes III and V are members of family 18. The two families share no sequence similarity. Within family 18 the class III plant chitinases show significant homology among themselves and with fungal chitinases; however, when the bacterial, insect and class V plant chitinases belonging to this family are included, the sequence similarity is restricted to two single conserved consensus regions of eight and nine residues respectively (Fig. 1) [8,9].

Until now only the three-dimensional (3D) structure of the family 19 chitinase from barley was known [10]. It consists of two domains with a fold related to that of the domains of animal and phage lysozymes [11]. Here, we present the crystal structure of hevamine, a class III chitinase from family 18.

Hevamine is a 29 kDa endochitinase that has been isolated from the vacuoles in the latex of the rubber tree (*Hevea brasiliensis*) [12]. In addition, hevamine exhibits lysozyme activity, as has been observed for several other chitinases [1]. The pH optimum of hevamine is 4.0 [12]. Its amino acid sequence [13] contains the two conserved

*Corresponding author.

		73	75	77	79		119	121	123	125	127	
Hevea	73	K	V	M	L	S	L	G	G	...	L	D	G	I	D	F	D	I	E	127
Cucumis	98	K	V	L	L	S	I	G	G	...	L	D	G	V	D	F	D	I	E	152
Nicotiana	89	K	T	F	L	S	I	A	G	...	F	H	G	L	D	L	D	W	E	138
Saccharomyces	102	K	V	L	L	S	L	G	G	...	V	D	G	F	D	F	D	I	E	157
Alteromonas	265	K	I	L	P	S	I	G	G	...	Y	D	G	V	D	I	D	W	E	313
Bacillus A1	158	K	T	I	I	S	V	G	G	...	F	D	G	V	D	L	D	W	E	204
Manduca sexta	257	K	F	M	V	A	V	G	G	...	F	D	G	L	D	L	D	W	E	146

Fig. 1. Comparison of the conserved regions in the amino acid sequences of selected family 18 chitinases. Sequence segments shown here are from *Hevea brasiliensis* hevamine [13], *Cucumis sativus* acidic chitinase [35], *Nicotiana tabaccum* class V chitinase [36], *Saccharomyces cerevisiae* chitinase [37], *Alteromonas* sp. chitinase 85 [15], *Bacillus circulans* chitinase A1 [14] and insect (*Manduca sexta*) chitinase [9]. Highly conserved amino acid residues are highlighted with shading.

family 18 consensus regions (Fig. 1). Site-directed mutagenesis studies performed with the homologous chitinase A1 of *Bacillus circulans* [14] and chitinase from *Alteromonas* [15] have shown that the glutamate residue in the consensus regions (Fig. 1) is essential for catalytic activity. This glutamic acid corresponds to Glu127 in hevamine. Mutation of the residue of the chitinase from *Alteromonas* [15] which is equivalent to Asp125 in hevamine also results in a complete loss of catalytic activity. However, this amino acid residue is not fully conserved in the chitinase family: the corresponding residue in the chitinase from *Arabidopsis thaliana* is an asparagine [16]. After mutation of the residues of chitinase A1 of *B. circulans* corresponding to Asp120 and Asp123 of hevamine, the bacterial chitinase still showed a residual activity. These findings indicate that the only conserved carboxylic group of the consensus regions that is essential for catalytic activity is the glutamic acid.

Hevamine is a fairly stable enzyme [12], and as such it offers a potential means to confer disease resistance upon plants. Moreover, family 18 chitinases are of very diverse origin (plants, fungi, bacteria, insects) and have widely differing properties with respect to pH optimum and reaction/substrate preference (endo- *versus* exo-chitinase activity; chitinase *versus* lysozyme activity). To understand this diversity in properties, it is essential to know the 3D structure. The structure presented here is the first structure of a member of family 18 of the glycosyl hydrolases, and is the first structure of a lysozyme or chitinase with a $(\beta\alpha)_8$-barrel fold. In addition, the 3D structure of the enzyme with a bound inhibitor is described. These structures establish a firm basis for the study of structure/function relationships among members of this family.

Results and discussion

Protein structure

As no homology was found with any protein with known structure [13], the X-ray structure of hevamine was determined by the method of multiple isomorphous replacement, and subsequently refined at 2.2 Å resolution to an R-factor of 16.9%. The enzyme comprises a single domain, which has a flattened ellipsoid shape, with approximate dimensions of 50 Å×40 Å×30 Å (Fig. 2). It has a $(\beta\alpha)_8$-barrel ('TIM barrel') folding motif (Fig. 3), which consists of an eight-stranded parallel β-barrel (β1–β8), surrounded by eight α-helices that are antiparallel to the barrel (α1–α8). Most connections between the carboxyl terminus of a helix and the amino terminus of a strand are 1–5 residues long; only one loop comprises 14 residues. The connections between the carboxyl terminus of a strand and the amino terminus of a helix are more variable in length, comprising 6–22 residues. Apart from the eight β-strands and eight α-helices of the $(\beta\alpha)_8$-barrel, the hevamine structure contains one extra helix after strand β8, and one extra strand located after strand β2, which form a two-stranded antiparallel β-sheet with the carboxy-terminal residues of β2. Three disulphide bridges are present, in agreement with the chemically determined connectivities [13]. The putative catalytic residue, Glu127, is located at the end of β4, with no other conserved aspartic or glutamic acid residues in its vicinity.

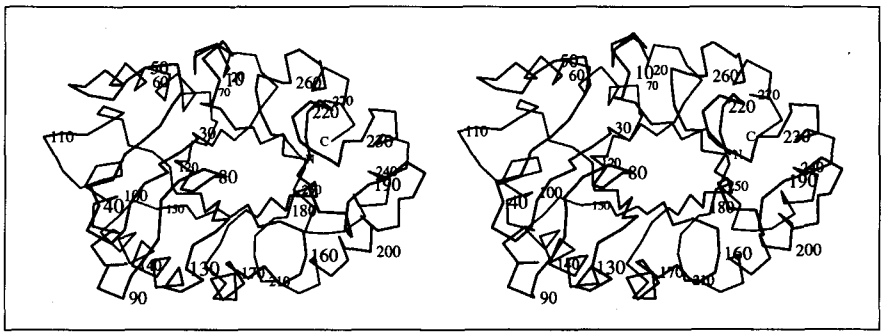

Fig. 2. Stereo Cα-trace of hevamine, with amino and carboxyl termini and every tenth residue labelled.

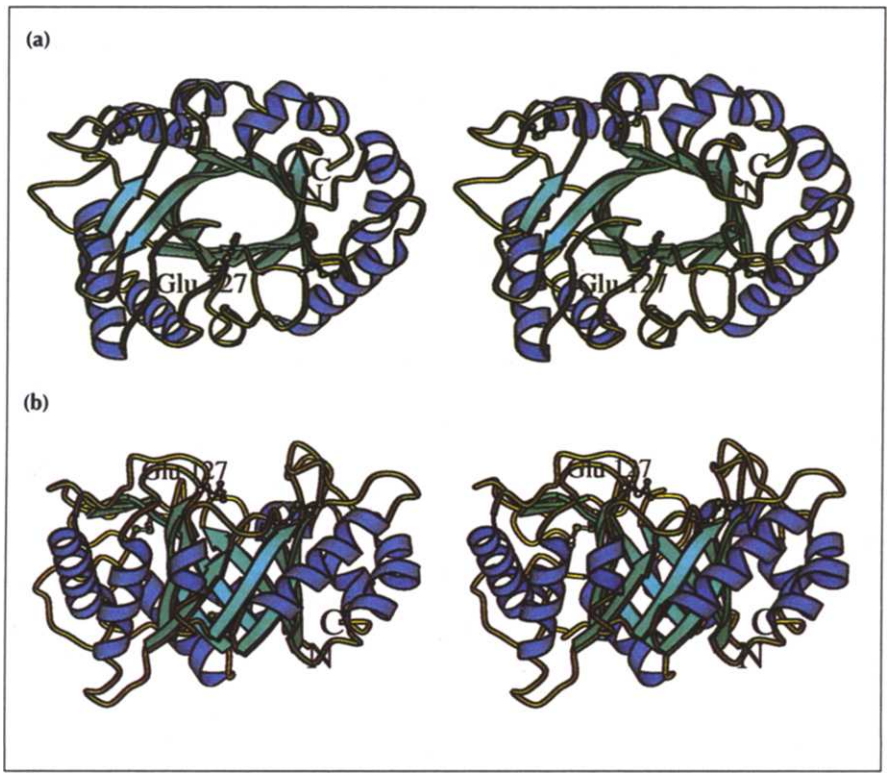

Fig. 3. A ribbon diagram of the structure of hevamine, drawn with the program MOLSCRIPT [38]. Strands are shown in cyan, helices in blue and loops in yellow. Cystine residues and the conserved Glu127 are shown in ball-and-stick representation. The amino and carboxyl termini are indicated. **(a)** Top view of the barrel. **(b)** Side view of the barrel, showing the cleft formed by the conserved loops at the carboxyl termini of the barrel strands.

The two family 18 consensus regions approximately correspond with the third and fourth strands of the β-barrel, residues 72–80 and 120–126 respectively. The β-strands form the interior of the protein and the conserved residues provide interactions with neighbouring strands (Fig. 4). The side chain of the absolutely conserved Asp123 makes hydrogen bonds with side chains of residues from β1, β3, β5 and β6, one of which is the highly conserved Ser77. Lys73 is close enough to Asp120 to make a salt bridge, but the lysine side chain is oriented in such a way that the contact between the two charges is formed via two solvent molecules. Although, at the pH of crystallization (pH 7.0), carboxylic groups are normally not protonated, the carboxylic group of the highly conserved Asp125 is within hydrogen-bonding distance of the putative catalytic Glu127. The latter residue is the first in the loop connecting β4 to α4. Asp125 is probably the proton donor for the hydrogen bond. As this residue is buried, and is close to the aromatic residues Tyr6 and Phe30, the hydrophobic environment of Asp125 is likely to raise its pK_a. Glu127 is more exposed to the solvent, and its pK_a is probably close to the typical value of 4.0–4.5 for carboxylic groups. The hydrogen bond might be necessary to orient the side chain of the putative catalytic Glu127 in the proper direction. The other conserved residues in the consensus regions are glycines, which are often close to bulky side chains. Whereas Gly121 has ϕ,ψ angles that are characteristic for a β-strand, the ϕ,ψ angles of Gly79 and Gly80 lie outside the regions allowed for other amino acid residues (Table 1). As most conserved residues in the consensus regions play a structural role in stabilizing the $(\beta\alpha)_8$-barrel, it is probable that all family 18 chitinases have a $(\beta\alpha)_8$-barrel domain.

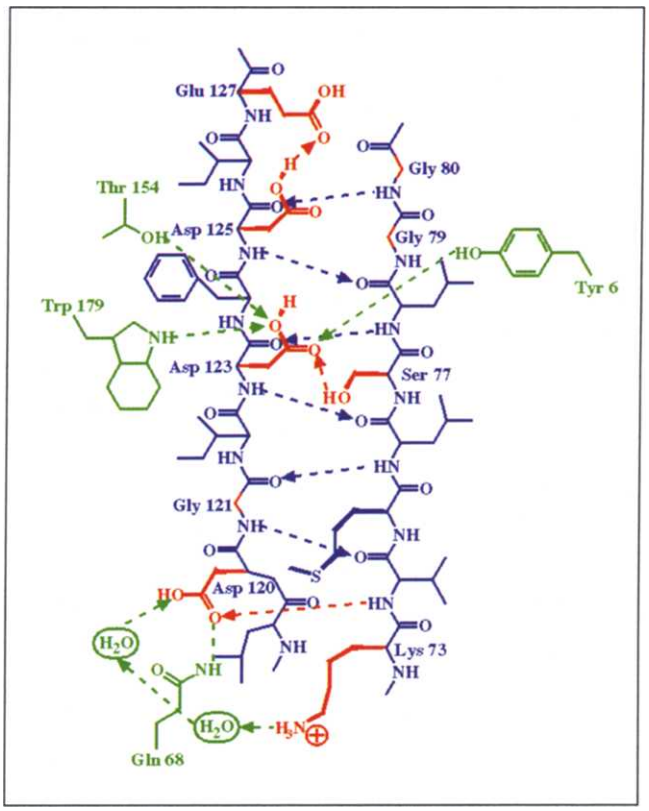

Fig. 4. Schematic drawing of the hydrogen-bonding pattern of the consensus regions. The highly conserved side chains and the hydrogen bonds that they make within the consensus regions are shown in red, the rest of the consensus regions are shown in blue. Hydrogen bonds made with residues outside the consensus regions are shown in green. Protonation of the side chains is shown to be most probable at pH 4.0, the pH optimum of hevamine.

Table 1. Dihedral angles of the glycine residues in the consensus regions.

	Φ	Ψ
Gly79	−178.3	−166.9
Gly80	104.4	−127.2
Gly121	103.5	178.3

Relationship to other chitinase and lysozyme structures

The only chitinase structure that has been published so far, the endochitinase from barley, is a family 19 chitinase [7]. Its fold shows clear similarities with goose lysozyme [11]. It consists of two domains, an α-helical and a mixed α/β-domain, with the substrate-binding cleft located between the two domains. Furthermore, structurally and catalytically important residues of the lysozyme superfamily are conserved in barley chitinase [11]. These include the catalytic glutamate and a glycine that is structurally important. The $(\beta\alpha)_8$-fold of hevamine is completely different from that of the barley chitinase and from the other known lysozyme folds, indicating that the two chitinase families have evolved from different ancestors.

Relationship with other $(\beta\alpha)_8$-barrel enzymes

Other polysaccharide-hydrolyzing enzymes that contain a $(\beta\alpha)_8$-barrel domain include α-amylase [17], β-amylase [18], cyclodextrin glycosyl transferase (CGTase) [19], cellobiohydrolase II [20] and barley β-glucanase [21]. These enzymes all have their active site at the carboxy-terminal end of the β-barrel, like hevamine, but the number and positions of the catalytic residues are quite diverse (Table 2). Furthermore, the other polysaccharide-hydrolyzing $(\beta\alpha)_8$-barrel enzymes all have extra domains, necessary for substrate binding. The only one that has its putative proton donor in the same loop as hevamine is β-amylase, but this enzyme needs two extra domains to bind its substrate. As the active site and mode of substrate binding of hevamine are different from that of the other enzymes, hevamine represents a new class of polysaccharide-hydrolyzing $(\beta\alpha)_8$-barrel enzymes.

From a structural point of view, the $(\beta\alpha)_8$-barrel structure of hevamine seems to be a member of family C, according to the classification of Farber and Petsko [22]. This family comprises single-domain $(\beta\alpha)_8$-barrel proteins that have their major β-barrel axis near β3. Furthermore, all members feature a small helix between β8 and α8. Among others, triosephosphate isomerase, *N*-(5′-phosphoribosyl) anthranilate isomerase, indole-3-glycerol-phosphate synthase and the α-subunit of tryptophan synthase belong in this family. The hevamine structure exhibits all the shared structural characteristics. However, none of the family C enzymes has a polysaccharide-hydrolyzing activity, and none of them has even hexose-binding capacity. Also, there are no obvious sequence similarities between hevamine and any of these enzymes. Moreover, they all use the positively charged main-chain nitrogen atoms of the extra helix after β8 for phosphate binding, whereas the same nitrogen in hevamine makes a hydrogen bond with a backbone oxygen of β1. This hydrogen bond seems to be of structural rather than functional importance. So, although there seems to be some structural resemblance between hevamine and the family C enzymes, no functional connection is apparent.

Location of the active site

In conformity with all known $(\beta\alpha)_8$-barrel enzymes, the active site of hevamine was expected to be located at the carboxy-terminal end of the β-barrel. In the hevamine structure the loops at this side of the barrel extend from the barrel strands to form a cleft ~30 Å long (Fig. 3).

Table 2. Features of glycosyl hydrolases with an $(\beta\alpha)_8$-barrel domain.

	Catalytic residues	Position[a]	Putative function	Cofactors	Position of extra domain
Cyclodextrin glycosyl-transferase [19,40]	Aspartic acid	β4	Stabilizing intermediate	2 Ca^{2+}	L3
	Glutamic acid	L5	Proton donor		Carboxy-terminal
	Aspartic acid	L7	Substrate binding		
α-amylase [17]	Aspartic acid	β4	Stabilizing intermediate	Ca^{2+}, Cl^-	L3
	Glutamic acid	L5	Proton donor		Carboxy-terminal
	Aspartic acid	L7	Substrate binding		
β-amylase [18]	Glutamic acid	L4	Proton donor	–	L3 and L4
Cellobiohydrolase II [20]	Aspartic acid	L2	Stabilizing intermediate	–	Amino-terminal
	Aspartic acid	L3	Proton donor		
β-glucanase [21]	Glutamic acid	β7	Stabilizing intermediate	–	L6
	Glutamic acid	α8	Proton donor		
Hevamine	Glutamic acid	L4	Proton donor	–	–

[a]Lx means the loop connecting βx with αx.

The loops are strongly conserved in plant and fungal chitinase sequences. Glu127, proposed to be essential for catalytic activity, is positioned just after β4. It forms part of the cleft (Fig. 3), which is consistent with this cleft forming the chitin-binding site.

To confirm that the active site is located near Glu127, we performed binding studies with *N,N′,N″*-triacetylchitotriose (tri-NAG), a chitin fragment (Fig. 5). Tri-NAG binds in the proposed binding cleft at three subsites, which we call A, B and C, with its reducing end at subsite C. The trisaccharide binds to the enzyme through both hydrogen bonds and van der Waals contacts. The hydrogen bonds are formed with the side chains of the residues Gln9, Asn45 and Trp255, which are conserved in plant and fungal chitinases, and with main-chain atoms. In contrast to many other saccharide-binding proteins [19,23], the van der Waals contacts are not formed by aromatic residues but by the side chains of Gln9, Ala47 and Ile82, of which only Gln9 is conserved (Fig. 6).

Beyond subsite C there seems to be space for three more subsites, which we call D, E and F. Three other *N*-acetylglucosamine moieties could be modelled in these proposed subsites; together with the bound trisaccharide, these allowed us to model a hexasaccharide in the active site (Fig. 7). The proposed subsites D, E and F are highly conserved in plant and fungal chitinases. The modelled saccharide residues can make hydrogen bonds to the conserved residues Gln158, Gln181, Tyr183, Asn184, Asn185 and Ala224. A seventh *N*-acetylglucosamine residue would probably not make any contacts with the protein, but is predicted to project into the solvent.

Glu127 is positioned between subsites D and E, with its Oε1 atom at hydrogen-bonding distance from the glycosidic oxygen between residues 4 and 5 of the modelled hexasaccharide. Glu127 is fixed in this position by a hydrogen-bonding interaction between its Oε2 and Asp125 (see above). The aspartate residues that are found in the conserved regions are too far away from the substrate to be directly involved in catalysis (Fig. 8); Asp125 is the nearest with a distance of 6.5 Å from the modelled hexasaccharide. At the pH optimum of the enzyme (pH 4.0), the side chain of Glu127 will be protonated. The glutamic acid would be in an excellent position to donate this proton to the glycosidic oxygen. If we assume that the first steps of the reaction mechanism are identical to those in hen egg-white lysozyme [24], proton donation would result in cleavage of the scissile bond and formation of a positively charged oxocarbonium intermediate. This intermediate needs to be attacked by a nucleophile to form the product. The most probable mechanism is an attack by an activated water molecule or a hydroxyl ion. If the water molecule were to attack the positively charged C1 of the intermediate from the side of the leaving group (the equatorial side) the configuration would be retained. In this case the intermediate would need to be stabilized until the leaving group has departed and a water molecule has entered the active site. In the case of hen egg-white

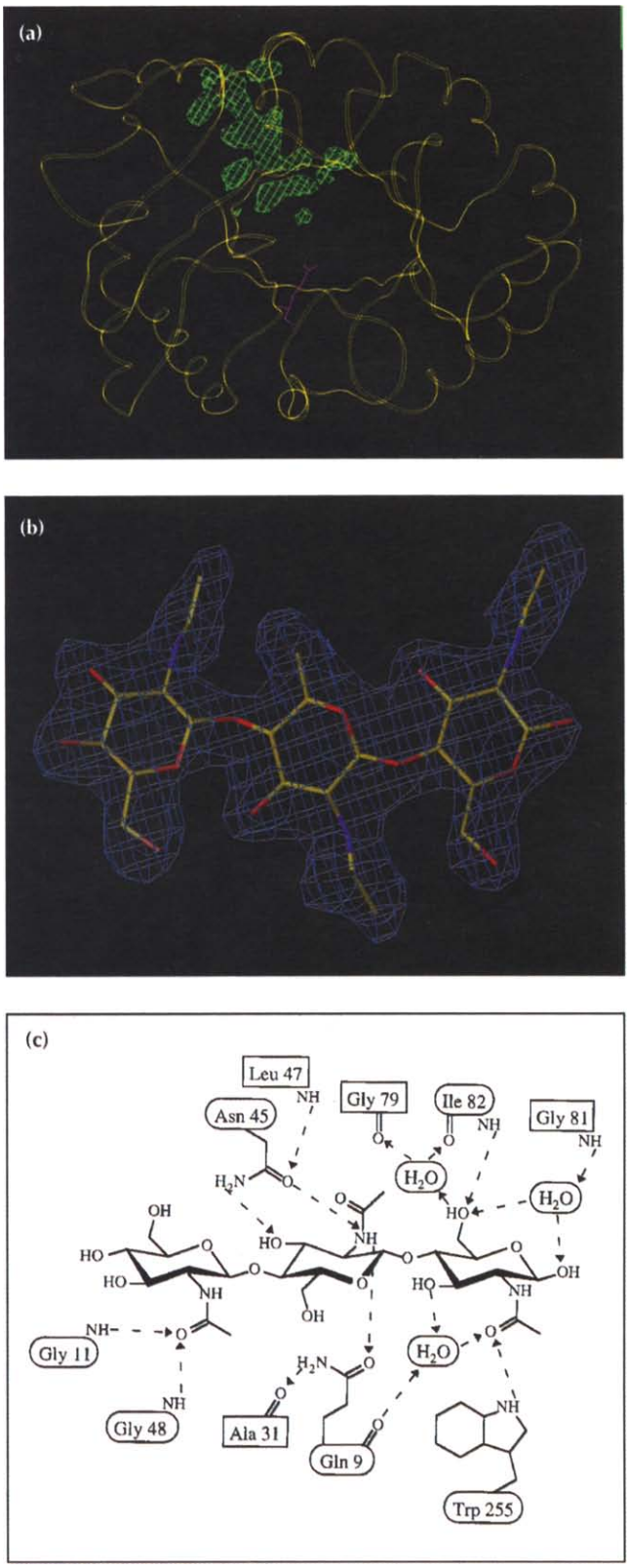

Fig. 5. (a) σ_A weighted F_o–F_c electron density [39] of tri-NAG bound to hevamine. Glu127 is shown in pink. **(b)** σ_A weighted $2F_o$–F_o electron density [39] of tri-NAG, with residue 1, which is bound at subsite A, oriented to the left. **(c)** Schematic drawing of the hydrogen-bonding contacts between the trisaccharide and hevamine, showing the residues of the first and second hydrogen-bonding shell with ellipsoid and rectangular boxes respectively.

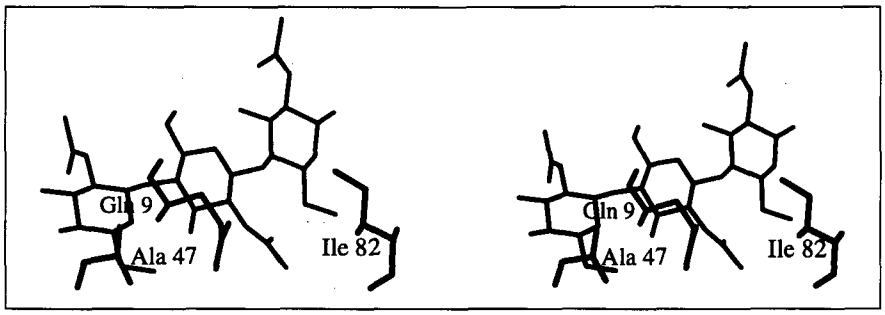

Fig. 6. Stereo figure showing the van der Waals interactions between hevamine and tri-NAG.

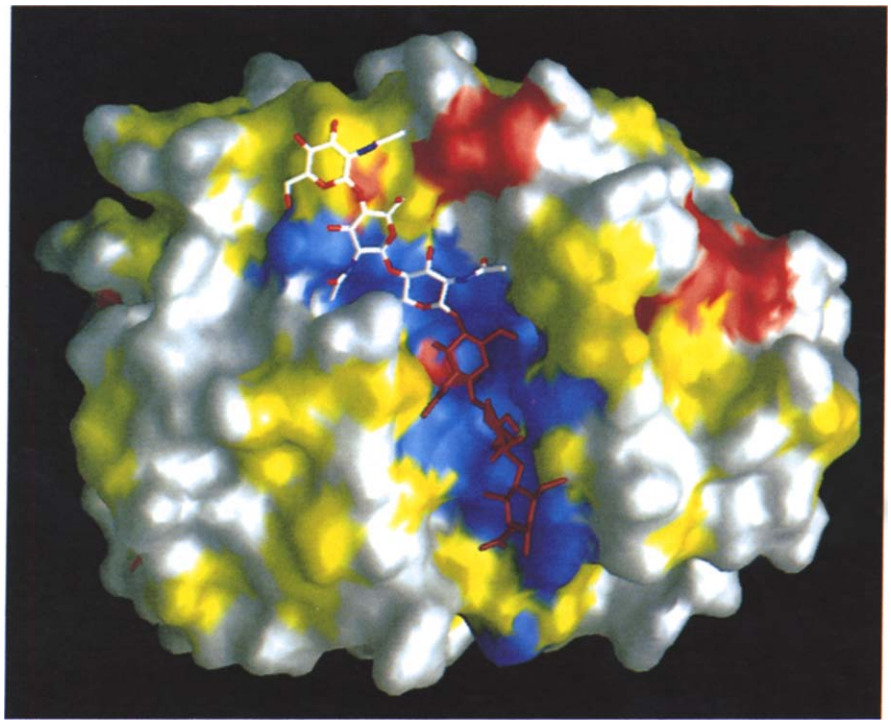

Fig. 7. Molecular-surface drawing of hevamine, in the same orientation as in Fig. 3a, created using GRASP (A Nicholls and B Honig, unpublished program). Colour coding is according to sequence conservation in all available class III plant and fungal chitinases (alignment not shown here). Blue corresponds to conserved side chains, red to side chains that are similar in all sequences, white to non-conserved side chains and yellow to main-chain atoms. The hexasaccharide is also shown, with the modelled residues in red.

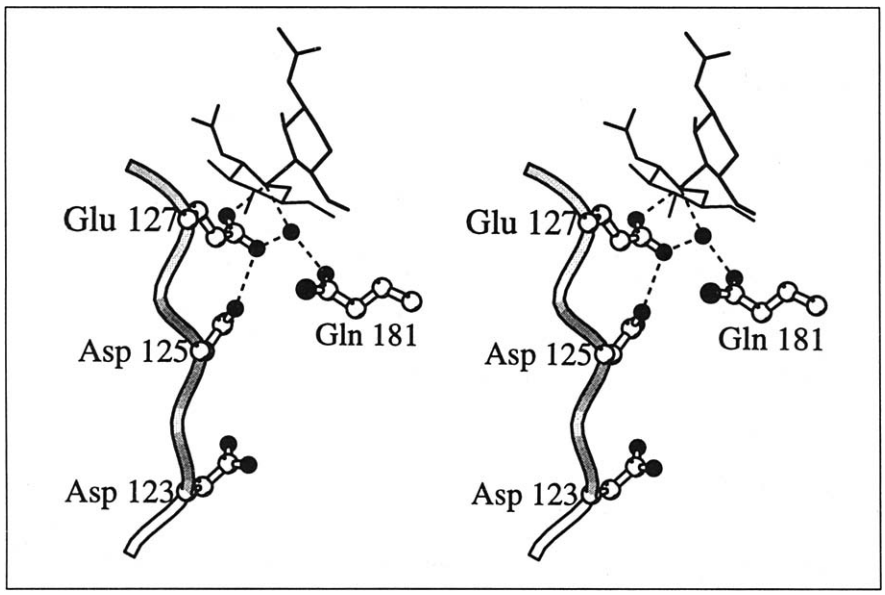

Fig. 8. Stereo drawing showing the geometry of the proposed active site. The modelled sugar residues 4 and 5, bound at subsites D and E are shown as a line drawing, and amino acid residues and the water molecule are shown in ball-and-stick representation. Atoms that are within hydrogen-bonding distance are connected by dashed lines.

lysozyme this stabilization would be provided by an aspartate residue. On the other hand, if a water molecule were to attack from the axial side, the configuration at the C1 atom of residue 4 would be inverted.

In hevamine, we could not find a negatively charged residue at an appropriate position to stabilize an oxocarbonium ion intermediate. However, a water molecule is found hydrogen bonded to the side chains of Gln181

(which is conserved in all plant and fungal chitinases) and Glu127 (Fig. 8). The water molecule is in the right position to attack the intermediate at the axial position, as it is <3 Å away from the C1 atom of the modelled residue 4. Although further experiments are needed, it seems likely that in the case of hevamine and related chitinases, inversion of configuration of the product at the C1 atom takes place.

Besides chitin, hevamine can hydrolyze the polysaccharide part of peptidoglycan. Whereas chitin is composed of linear chains of *N*-acetylglucosamine residues, peptidoglycan consists of alternating *N*-acetylglucosamine and *N*-acetylmuramic acid residues. *N*-acetylmuramic acid differs from *N*-acetylglucosamine by the presence of a lactyl group (to which a peptide crosslink may be attached) bound to the O3 atom. In peptidoglycan, each sugar residue is rotated by ~45° [25], causing the muramic acid residues (and thus the crosslinks) to be rotated by 90° with respect to each other.

As the tri-NAG binds with the plane of the sugar rings parallel to the bottom of the substrate-binding cleft, all three O3 atoms point towards the solvent. Thus, *N*-acetylmuramic acid can bind at positions A, B and C. This indicates that, in contrast to hen egg-white lysozyme, which has the substrate bound with the plane of the sugar rings perpendicular to the bottom of the substrate-binding cleft, hevamine shows no specificity towards one mode of peptidoglycan binding, although the glycan has to undergo some strain to adopt a flat position similar to the tri-NAG. However, the O3 of the modelled sugar residue at subsite F points into the cleft, as it hydrogen bonds to the Oϵ1 of Gln158, so that *N*-acetylmuramic acid probably is not able to fit at this subsite. If it is necessary for the catalytic activity to have subsite F occupied, this would imply that hevamine binds the peptidoglycan preferentially with an *N*-acetylglucosamine residue at site D and an *N*-acetylmuramic acid residue at site E, which would be different from the specificity of hen egg-white lysozyme [24], and also from two other plant lysozymes that have been investigated [26,27].

Biological implications

Hevamine is a plant enzyme with chitinase and lysozyme activities. Chitinases are key enzymes in plant defence mechanisms against pathogenic fungi. As chitinases even within the same family show widely differing properties with respect to pH optimum, substrate specificity (e.g. chitinase *versus* lysozyme activity) and reaction specificity (endochitinase *versus* exochitinase activity) a complete understanding of these properties requires knowledge of the three-dimensional structure. Hevamine shows sequence similarities with several chitinases from plants, fungi, insects and bacteria but not with other investigated lysozymes and the related barley chitinase. Also, it is significantly larger (29 kDa) than animal and phage lysozymes (14–21 kDa).

The three-dimensional structure described here shows the fold of hevamine to be a $(\beta\alpha)_8$-barrel motif. The substrate-binding site was located by binding of a chitin fragment. The active site is near Glu127, which is in a good position to act as the catalytic acid in the hydrolysis reaction. However, no residue is in a position to stabilize a resulting positively charged oxocarbonium ion intermediate. Instead, a water molecule is bound close to the axial side of the C1 atom of the scissile bond in a modelled substrate, implying that no long-lived intermediate is necessary and that the reaction will proceed with inversion of the configuration at C1.

Hevamine is a member of a family of chitinases produced by a wide range of organisms. Because many residues that are conserved in this family stabilize the $(\beta\alpha)_8$-barrel in hevamine, it is likely that all members of the family contain a $(\beta\alpha)_8$-barrel domain. As the fold is completely different from other known lysozymes and chitinases, this class must have evolved independently.

The crystal structure of hevamine helps explain the results of site-directed mutagenesis studies performed on homologous bacterial chitinases, and provides an important tool for engineering substrate specificity and catalytic properties.

Materials and methods

Crystals were grown from 20% (w/v) NaCl as described previously [28]. They are in space group $P2_12_12_1$ with cell dimensions a=52.3 Å, b=57.7 Å and c=82.1 Å. Each asymmetric unit contains one molecule of hevamine. A native data set was collected to 2.2 Å (Native 1).

For the heavy-atom screening the crystals were transferred to a mother liquor containing 23% (w/w) polyethylene glycol (PEG) 6000 at pH 9.5. With the original mother liquor, none of over 60 compounds, tested at four different pH values, resulted in differences in the diffraction pattern. Four out of six compounds tested with the new mother liquor yielded usable derivatives: these were saturated 2,4-dichloromercuri-6-nitrophenol (Hg 1), 10 mM $(CH_3)_3PbAc$ (Pb), 5 mM 4-acetamidophenyl-mercuric acetate (Hg 2) and 20 mM $AgNO_3$ (Ag). The Hg 1 and Pb derivatives gave interpretable difference Patterson maps; the resulting phases helped in interpreting the Hg 2 and Ag data. All data were collected on an Enraf Nonius FAST area detector, with CuKα X-rays from an Elliot GX21 rotating anode generator. As the diffraction pattern of native crystals changed slightly upon the transfer to PEG 6000, a native data set to 2.65 Å was collected from a crystal soaked in the new mother liquor (Native 2).

Data were processed with MADNES [29], with XDS profile fitting [30]. Using the Native 2 data, phases were determined with the program PHARE [31], and improved by solvent flattening [32] (Table 3). The structure was built using O [33]. Alternating cycles of model building and energy minimization with X-PLOR of partial models against Native 2 resulted in a complete model. This model was subsequently refined against

the Native 1 data by simulated annealing with X-PLOR [34]. The current model, which is refined to 2.2 Å, comprises all 273 residues and 249 water molecules. Details on the quality of the model are shown in Table 3 and Fig. 9.

Crystals of the hevamine–trisaccharide complex were obtained by soaking native hevamine crystals in a mother liquor containing 20% (w/v) NaCl and 30 mM tri-NAG at pH 9.5, which caused the cell dimensions to change slightly. The trisaccharide was built in a difference Fourier electron-density map, using the native hevamine structure as a starting model. The model was also refined using X-PLOR [34]. Details of the data collection and the quality of the model are shown in Table 3.

Modelling of the hexasaccharide was performed with the energy-minimization option of BIOGRAF (obtained from Molecular Simulations Inc., Waltham, MA, USA).

Table 3. Data collection, phase determination and refinement.

Crystal/derivative	Native 1	Native 2	Hg 1	Pb	Hg 2	Ag	Tri-NAG
Data							
Resolution (Å)	15–2.2	28–2.65	10–2.65	15–2.65	8–2.65	25–4	28–2.4
Number of unique reflections	11 451	7040	6464	6200	5849	1769	9453
Completeness	0.871	0.928	0.897	0.871	0.861	0.916	0.926
R_{merge}[a]	0.052	0.030	0.054	0.052	0.055	0.058	0.082
R_{native}[b]	0.104		0.148	0.243	0.283	0.190	0.204[c]
MIR analysis							
Number of sites			1	1	4	2	
Phasing power[d]			1.70	1.35	1.55	1.45	
Structure refinement							
Resolution (Å)	8.0–2.2						8.0–2.4
Number of unique reflections	11 241						9145
Number of water molecules	249						204
R-factor[e]	0.169						0.144
Rms Δ bond lengths (Å)	0.014						0.015
Rms Δ bond angles (°)	3.0						3.1
Rms Δ B main-chain atoms (Å^2)	1.29						1.38
Rms Δ B side-chain atoms (Å^2)	2.26						2.32

[a] $R_{merge} = \Sigma|I(hkl,j) - <I(hkl)>|/\Sigma<I(hkl)>$. [b] $R_{native} = \Sigma|F_1 - F_2|/\Sigma F_1$, with F_2 referring to data set Native 2. [c] R_{native}, but with F_2 referring to data set Native 1. [d] Phasing power is the mean value of the heavy atom structure amplitude divided by the residual lack of closure error. [e] R-factor $= \Sigma|F_o - F_c|/\Sigma F_o$. Native 1 was collected from a crystal with the standard mother liquor containing 20% NaCl at pH 7.0. Native 2 and the derivative data sets were collected from crystals from mother liquors containing 20% (w + v) PEG-6000 at pH 9.5 plus saturated 2,4-dichlqromercuri-6-nitrophenol (Hg 1), or 10 mM $(CH_3)_3PbAc$ (Pb), or 5 mM 4-acetamido-phenyl-mercuric acetate (Hg 2) or 20 mM $AgNO_3$ (Ag). Tri-NAG is a data set collected from a crystal soaked in a mother liquor containing 23% (w/w) PEG-6000 and 30 mM *N,N′,N″*-triacetylchiotriose (tri-NAG) at pH 9.5.

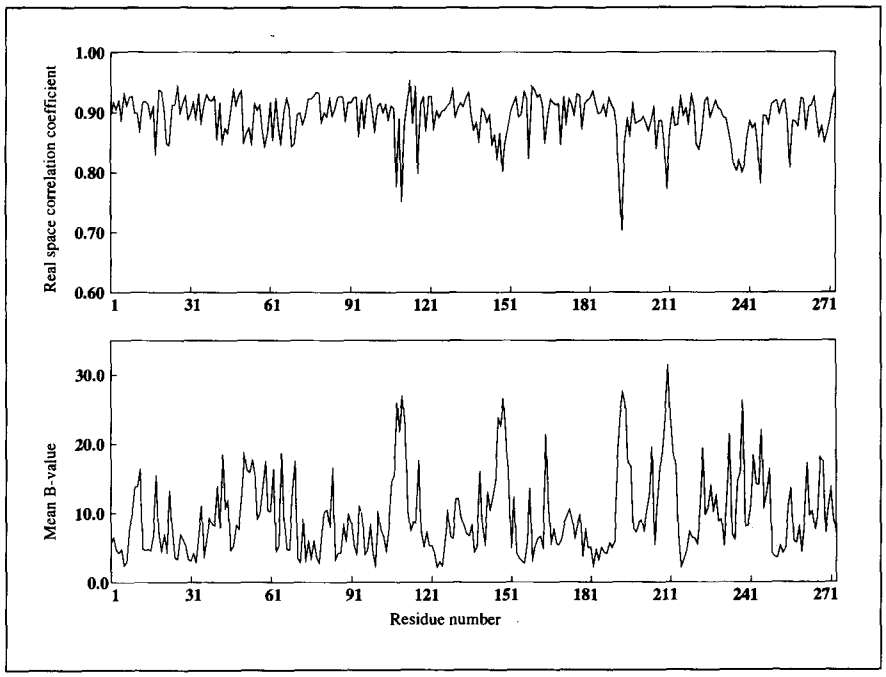

Fig. 9. Average real-space correlation coefficients [33] and temperature factors for all hevamine atoms of the refined 2.2 Å resolution model. The minima in the real-space fit (<0.80) coincide with maxima in temperature factors, and correspond to exposed loop regions.

Atomic coordinates for the native enzyme and the complex are being deposited with the Brookhaven Protein Data Bank (tracking numbers T5466 and T5467 respectively).

Note added in proof

In this issue of *Structure* the crystal structure of a bacterial chitinase is discussed. It consists of three domains; the catalytic domain contains the family 18 consensus regions and has a $(\beta/\alpha)_8$-barrel fold [Perrakis, A., *et al.*, & Vorgias, C.E. (1994). Crystal structure of a bacterial chitinase at 2.3 Å resolution. *Structure* **2**, (1169–1180)].

References

1. Sahai, A.S. & Manocha, M.S. (1993). Chitinases of fungi and plants — their involvement in morphogenesis and host parasite interaction. *FEMS Microbiol.* Rev. **11**, 317–338.
2. Collinge, D.B., Kragh, K.M., Mikkelsen, J.D., Nielsen, K.K., Rasmussen, U. & Vad, K. (1993). Plant chitinases. *Plant J.* **3**, 31–40.
3. Schlumbaum, A., Mauch, F., Vögeli, U. & Boller, T. (1986). Plant chitinases are potent inhibitors of fungal growth. *Nature* **324**, 365–367.
4. Lamb, C.J., Ryals, J.A., Ward, E.R. & Dixon, R.A. (1992). Emerging strategies for enhancing crop resistance to microbial pathogens. *Biotechnology* **10**, 1436–1445.
5. Beintema, J.J. (1994). Structural features of plant chitinases and chitin-binding proteins. *FEBS Lett.* **350**, 159–163.
6. Henrissat, B. (1991). A classification of glycosyl hydrolases based on amino acid sequences. *Biochem. J.* **280**, 309–316.
7. Henrissat, B. & Bairoch, A. (1993). New families in the classification of glycosyl hydrolases based on amino acid sequence similarities. *Biochem. J.* **293**, 781–788.
9. Kramer, K.J., Corpuz, L., Choi, H.K. & Muthukrishnan, S. (1993). Sequence of a cDNA and expression of the gene encoding epidermal and gut chitinases of *Manduca sexta*. *Insect Biochem. Mol. Biol.* **23**, 691–701.
10. Hart, P.J., Monzingo, A.F., Ready, M.P., Ernst, S.R. & Robertus, J.D. (1993). Crystal structure of an endochitinase from *Hordeum vulgare* L. seeds. *J. Mol. Biol.* **229**, 189–193.
11. Holm, L. & Sander, C. (1994). Structural similarity of plant chitinase and lysozymes from animals and phage — an evolutionary connection. *FEBS Lett.* **340**, 129–132.
12. Tata, S.J., Beintema, J.J. & Balabaskaran, S. (1983). The lysozyme of *Hevea brasiliensis* latex: isolation, purification, enzyme kinetics and a partial amino-acid sequence. *J. Rubb. Res. Inst. Malaysia* **31**, 35–48.
13. Jekel, P.A., Hartmann, J.B.H. & Beintema, J.J. (1991). The primary structure of hevamine, an enzyme with lysozyme/chitinase activity from *Hevea brasiliensis* latex. *Eur. J. Biochem.* **200**, 123–130.
14. Watanabe, T., *et al.*, & Tanaka, H. (1993). Identification of glutamic acid-204 and aspartic acid-200 in chitinase-A1 of *Bacillus circulans* WL-12 as essential residues for chitinase activity. *J. Biol. Chem.* **268**, 18567–18572.
15. Tsujibo, H., Orikoshi, H., Imada, C., Okami, Y., Miyamoto, K. & Inamori, Y. (1993). Site-directed mutagenesis of chitinase from *Alteromonas* sp. strain o-7. *Biosci. Biotechnol. Biochem.* **57**, 1396–1397.
16. Samac, D.A., Hironaka, C.M., Yallaly, P.E. & Shah, D.M. (1990). Isolation and characterization of the genes encoding basic and acidic chitinase in *Arabidopsis thaliana*. *Plant Physiol.* **93**, 907–914.
17. Qian, M., Haser, R., Buisson, G., Duée, E. & Payan, F. (1994). The active center of a mammalian α-amylase. Structure of the complex of a pancreatic α-amylase with a carbohydrate inhibitor refined to 2.2 Å resolution. *Biochemistry* **33**, 6284–6294.
18. Mikami, B., *et al.*, & Morita, Y. (1992). Three-dimensional structure of soybean beta-amylase determined at 3.0 Å resolution: preliminary chain tracing of the complex with alpha-cyclodextrin. *J. Biochem.* **112**, 541–546.
19. Lawson, C.L., *et al.*, & Dijkstra, B.W. (1994). Nucleotide sequence and X-ray structure of cyclodextrin glycosyl transferase from *Bacillus circulans* strain 251 in a maltose-dependent crystal form. *J. Mol. Biol.* **236**, 590–600.
20. Rouvinen, J., Bergfors, T., Teeri, T., Knowles, J.K.C. & Jones, T.A. (1990). Three-dimensional structure of cellobiohydrolase II from *Trichoderma reesei*. *Science* **249**, 380–386.
21. Varghese, J.N., Garrett, T.P.J., Colman, P.M., Chen, L. & Høj, P.B. (1994). Three-dimensional structure of two plant beta-glucan endohydrolases with distinct substrate specificities. *Proc. Natl. Acad. Sci. USA* **91**, 2785–2789.
22. Farber, G.K. & Petsko, G.A. (1990). The evolution of alpha/beta barrel enzymes. *Trends Biochem. Sci.* **15**, 228–234.
23. Quiocho, F.A. (1989). Protein–carbohydrate interactions: basic molecular features. *Pure & Appl. Chem.* **61**, 1293–1306.
24. Strynadka, N.C.J. & James, M.N.G. (1991). Lysozyme revisited: crystallographic evidence for distortion of an *N*-acetylmuramic acid residue bound in site D. *J. Mol. Biol.* **220**, 401–424.
25. Labischinski, H. & Maidhof, H. (1994). Bacterial peptidoglycan: overview and evolving concepts. In *Bacterial Cell Wall.* (Ghuysen, J.-M. & Hakenbeck, R., eds), pp. 23–38, Elsevier, Amsterdam.
26. Howard, J.B. & Glazer, A.N. (1969). Papaya lysozyme, terminal sequences and enzymatic properties. *J. Biol. Chem.* **244**, 1399–1409.
27. Audy, P., Trudel, J. & Asselin, A. (1988). Purification and characterization of a lysozyme from wheat germ. *Plant Sci.* **58**, 43–50.
28. Rozeboom, H.J., Budiani, A., Beintema, J.J. & Dijkstra, B.W. (1990). Crystallization of hevamine, an enzyme with lysozyme/chitinase activity from *Hevea brasiliensis* latex. *J. Mol. Biol.* **212**, 441–443.
29. Messerschmidt, A. & Pflugrath, J.W. (1987). Crystal orientation and X-ray pattern prediction routines for area-detector diffractometer systems in macromolecular crystallography. *J. Appl. Crystallogr.* **20**, 306–315.
30. Kabsch, W. (1988). Evaluation of single-crystal X-ray diffraction data from a position-sensitive detector. *J. Appl. Crystallogr.* **21**, 916–924.
31. Bricogne, G. (1976). Methods and programs for direct-space exploitation of geometric redundancies. *Acta Crystallogr. A* **32**, 832–847.
32. Wang, B.C. (1985). Resolution of phase ambiguity in macromolecular crystallography. *Methods Enzymol.* **115**, 90–112.
33. Jones, T.A., Zou, J.-Y., Cowan, S.W. & Kjeldgaard, M. (1991). Improved methods for building protein models in electron density maps and the location of errors in these models. *Acta Crystallogr. A* **47**, 110–119.
34. Brünger, A.T., Kuriyan, J. & Karplus, M. (1987). Crystallographic R-factor refinement by molecular dynamics. *Science* **235**, 458–460.
35. Metraux, J.P., *et al.*, & Ryals, J. (1989). Isolation of a complementary DNA encoding a chitinase with structural homology to a bifunctional lysozyme/chitinase. *Proc. Natl. Acad. Sci. USA* **86**, 896–900.
36. Melchers, L.S., *et al.*, & Linthorst, H.J.M. (1994). A new class of tobacco chitinases homologous to bacterial exo-chitinases displays antifungal activity. *Plant J.* **5**, 469–480.
37. Kuranda, M.J. & Robbins, P.W. (1991). Chitinase is required for cell separation during growth of *Saccharomyces cerevisiae*. *J. Biol. Chem.* **266**, 19758–19767.
38. Kraulis, P.J. (1991). MOLSCRIPT: a program to produce both detailed and schematic plots of protein structures. *J. Appl. Crystallogr.* **24**, 946–950.
39. Read, R.J. (1986). Improved Fourier coefficients for maps using phases from partial structures with errors. *Acta Crystallogr. A* **42**, 140–149.
40. Strokopytov, B., Penninga, D., Rozeboom, H.J., Kack, K.H., Dijkhuizen, L. & Dijkstra, B.W. (1995). X-ray structure of cyclodextrin glycosyltransferase complexed with acarbose. Implications for the catalytic mechanism of glycosidases. *Biochemistry*, in press.

Received: **17 Aug 1994**; revisions requested: **7 Sep 1994**; revisions received: **21 Sep 1994**. Accepted: **3 Oct 1994**.